Local Structure around Iron Ions in Anatase TiO_2

Sanyuan Zhu[2], Wenhan Liu[2], Shiqiang Wei[4], Chongzheng Fan[3], and Yuzhi Li[1]

[1]*Structure Research Laboratory,* [2]*Department of Physics,* [3]*Department of Chemical Physics,*
[4]*National Synchrotron Radiation Laboratory,*
University of Science and Technology of China, Hefei 230026, People's Republic of China

Abstract. The local structure around iron impurity in anatase TiO_2 nano-composite with different iron content (1, 2, 5 and 10 wt %) has been studied by fluorescence XAFS. The results indicate that for the sample with low iron content (1 and 2 wt %), the iron ions are incorporated into the lattice of anatase, and substitute the Ti ions. With the iron content increasing to 5 wt %, only part of iron ions enter the lattice of anatase, and the rest form α-Fe_2O_3 phase. As the iron content reaches 10 wt %, iron ions mainly exist in α-Fe_2O_3 phase. It is found that, in the (1 wt %)Fe-doped TiO_2 the bond lengths of the first (Fe-O) and second (Fe-Ti) shells are $R_{Fe\text{-}O}$=1.97 Å and $R_{Fe\text{-}Ti}$=3.01 Å, respectively, which means that the $R_{Fe\text{-}O}$ is only slightly larger than the first shell Ti-O bond length by 0.01 Å, while the $R_{Fe\text{-}Ti}$ is significantly smaller (0.04 Å) than that of the corresponding Ti-Ti shell in anatase. These results imply that iron ions occupying the Ti sites greatly change the symmetry of the first Fe-O shell.

Keywords: Fe-doped TiO_2; XAFS
PACS: 61.10.Ht; 61.72.Ww

INTRODUCTION

Diluted magnetic semiconductors have received considerable attention because of combined magnetic and transport properties as well as their easy integration into existing semiconductor devices, which are desirable for spintronics applications [1-2]. Electronic structure calculations indicate that alternative dopants such as Co, Fe and Mn may be ferromagnetic in TiO_2 [3]. Recently Wang *et al.* claimed that they have obtained a room temperature diluted magnetic semiconductors in Fe-doped rutile thin films prepared by plasma laser deposition [4]. Suryanrayanan *et al.* reported that Fe-doped anatase and rutile TiO_2 films on sapphire substrates prepared by the spin-on technique have a Curie temperature as high as 400 K [5]. However, the magnetic moments per Fe atom in these reports are far different from each other, ranging from 0.14 [6] via 0.46 [5] to 2.4 [4] μ_B per Fe atoms. Paramagnetism was also reported in this system. Wang *et al.* reported that Fe-doped nano-powders with iron content from 0 to 16.7 at%, synthesized using oxidative pyrolysis of liquid-feed metal organic precursors in radiation-frequency thermal plasma, are paramagnetic at room temperature [7]. Similar results were reported by Bally *et al.* [8]. Additionally, Kim *et al.* reported that the room temperature ferromagnetism of Fe-doped TiO_2 film with 7 at% Fe atoms grown by oxygen-plasma-assisted molecular beam epitaxy is associated with the presence of Fe_3O_4 [9]. To better understand the magnetic properties of Fe doped TiO_2, we present a direct determination of the local structure around iron ions in anatase TiO_2, using Fe-K edge EXAFS. The results show that Fe^{3+} ions enter the anatase lattice and substitute Ti^{4+} ions up to 2 wt% in nano-powder samples, and the presence of α-Fe_2O_3 is apparent for samples with higher concentration.

EXPERIMENTAL

Fe-doped TiO_2 nano-powders, with iron contents 1, 2, 5 and 10 wt%, respectively, were prepared by sol-gel method. All powders were sintered in air at 923 K for 10 h [10]. X-ray absorption measurements of the Fe-doped TiO_2 nano-powders were performed at the 4W1B of Beijing Synchrotron Radiation Facility (BSRF). The storage ring was run at 2.2 GeV with a maximum current of 100 mA. Fixed-exit Si(111) flat double crystals were used as monochromator. XAFS spectra at the Fe K-edge of the samples with 1, 2, and 5 wt % iron content were collected with a fluorescence ionization chamber filled with Ar at room temperature, while the XAFS spectra of 10 wt% Fe-doped TiO_2 and the α-Fe_2O_3 powder, and the Ti K-edge XAFS spectra of anatase powder were collected in transmission mode.

RESULTS AND DISCUSSION

The EXAFS functions $k^3\chi(k)$ and their Fourier transforms (FT) for α-Fe_2O_3, anatase TiO_2 and Fe-doped TiO_2 nano-composites are shown in Figs. 1 and 2, respectively. The FT was performed using a k region of 2.5-11.3 $Å^{-1}$ and a Hanning window. Several strong oscillations appear in the high k region for the α-Fe_2O_3 powder (Fig. 1). Especially, the strong oscillation A at k=7.6 $Å^{-1}$ in the $k^3\chi(k)$ function of the α-Fe_2O_3 powder is a characteristic of the trigonal structure, while it disappears for the distorted octahedron structure of anatase. For Fe-doped TiO_2 composites, this peak gradually decreases in amplitude with reduced iron concentration. At the 1-wt% Fe concentration, peak A disappears, similar for that of the anatase powder.

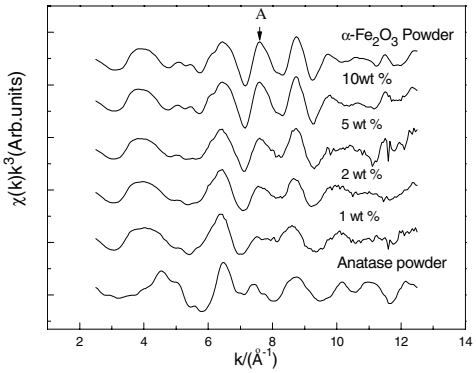

FIGURE 1. The $k^3\chi$ (k) functions of the α-Fe_2O_3, anatase powder and Fe-doped TiO_2 composites with different iron concentrations.

Figure 2 demonstrates that there are three strong peaks located at 1.5, 2.5 and 3.1 Å in the FT of the α-Fe_2O_3 powder. The first and second peaks correspond to the first shell of three Fe-O pairs with bond length of 1.94 Å, the second shell of three Fe-O pairs with bond length of 2.11 Å and four Fe-Fe pairs with bond length of 2.90 Å. For the anatase powder there are also three strong peaks located at 1.5, 2.6 and 3.2 Å in the FT. The first peak corresponds to the first shell of four Ti-O pairs with bond length of 1.94 Å, the second shell of two Ti-O pairs with bond length of 1.97 Å and four Ti-Ti pairs with bond length of 3.1 Å. Though three strong peaks appear in the FT of both α-Fe_2O_3 and anatase, the intensity and shape for these peaks are quite distinct from each other. The first peak in the FT of anatase is much higher than that of α-Fe_2O_3, while the second peak shows the opposite character. Moreover, the shape in higher R range is also quite different. These results show that the character of the FT can distinguish iron atoms existing in α-Fe_2O_3 phase from those entering the anatase lattice. For Fe-doped TiO_2 with 10 wt% iron content, the FT is almost the same as that of α-Fe_2O_3. With reduced iron concentration, the intensity of the first peak increases slightly, while the intensity of the second peak decreases. The shape in the high R range also changes. With the Fe concentration reaching 1 wt%, the character of the FT is very similar to that of the anatase powder. From the similarity of the FTs, it is concluded that for the samples with low iron content (1 and 2 wt%), the iron ions are incorporated into the anatase lattice, and substitute the Ti ions. With the iron content increasing to 5 wt %, only part of iron ions enter the lattice of anatase, and the rest form α-Fe_2O_3 phase. At 10 wt%, iron ions mainly exist in α-Fe_2O_3 phase.

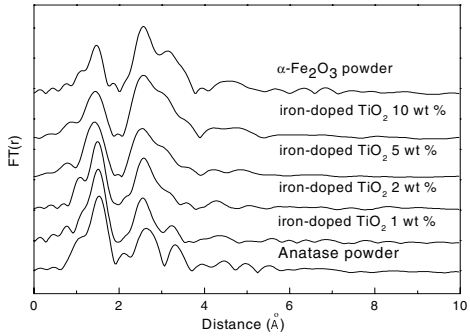

FIGURE 2. Rhe RSF curve of the α-Fe_2O_3, anatase powder and Fe-doped TiO_2 composites with different iron concentrations.

To obtain the structure parameters of iron entering the anatase lattice, least-squares curve fits were performed using the UWXAFS3.0 code, based on the single-scattering theory. S^2_0 was obtained from fitting the curve of α-Fe_2O_3. The curve fits of 1 wt% Fe-doped TiO_2 was performed in the R range 0.9-3.1 Å for the first nearest Fe-O shell (R_{eff} =1.94 Å) and one second Fe-Ti shell (R_{eff} =3.04 Å). The fitting results are summarized in Table 1.

TABLE 1. Local structure parameters of anatase powder and Fe-doped TiO_2 with 1 wt% iron.

sample	Shell	N	R(Å)	σ^2 ($Å^2$)	ΔE (eV)
TiO2	Ti-O	6.0	1.96	0.0060	-3.9
	Ti-Ti	4.0	3.05	0.0075	-3.9
1 wt %	Fe-O	6.4	1.97	0.0065	-6.5
	Fe-Ti	3.8	3.01	0.0071	-6.5

As seen from Table1, the coordination numbers N of the first-nearest and second-nearest shell are almost the same between 1 wt% Fe-doped TiO_2 and the anatase powder. This indicates that no oxygen vacancy exists around iron ions in the 1 wt% Fe-doped TiO_2. The Fe-O bond length in Fe-doped TiO_2

with 1 wt% iron is only 0.01 Å larger than the Ti-O bond length in the anatase powder, while the Fe-Ti bond length in Fe-doped TiO_2 with 1 wt% iron is 0.04 Å smaller than the Ti-O bond length in the anatase powder. The abnormal bond length variation of the Fe-O and Fe-Ti shells indicates that iron ions substituting the Ti ions greatly affect the symmetry of the first Fe-O shell, and the O-Fe-O bond angle in 1 wt% Fe-doped TiO_2 is probably changed, compared with the O-Ti-O angle in the anatase powder. It is noteworthy that in Fig. 1 the oscillations in the low k region (k<6 Å^{-1}) of the $k^3\chi(k)$ function for Fe-doped TiO_2 with 1 wt % are quite different from those for the anatase powder. This also confirms that iron ions have notably changed the local structure around iron ions. Moreover, one can see that the oscillations in the low k region (k<6 Å^{-1}) of the $k^3\chi(k)$ function for Fe-doped TiO_2 with 1 wt% are similar to those for the α-Fe_2O_3 powder. We consider that the symmetry of the first O shell around iron ions is probably the same between 1 wt% Fe-doped TiO_2 and the α-Fe_2O_3 powder, with different distance of the Fe-O bond.

In the EXAFS analysis, the consideration of iron ions substituting the Ti ions is based on the similarity of the RSF curve between 1 wt% Fe-doped TiO_2 and the anatase powder. To further verify this point, the following reasons are given. Mössbauer spectra [10] results indicate that iron ions in Fe-doped TiO_2 are Fe^{3+}; therefore iron metal, FeO and Fe_3O_4 are ruled out. Moreover, the RSF results of γ-Fe_2O_3 and Fe_2TiO_5–based models (calculated by using the FeFF7 [12]) show completely different characters from the RSF curve of 1 wt% Fe-doped TiO_2. These results indicate that it is impossible that iron ions in 1 w% Fe-doped TiO_2 exist as these iron compounds. Suryanrayanan *et al.* [5], Wang *et al.* and Hong *et al.* have claimed that Fe ions substitute the Ti ions in the Fe-doped TiO_2 for iron content up to 8 %, since no peaks of iron clusters or iron oxides are observed in their XRD patterns. Our previous studies have obtained similar XRD results in 10 wt% Fe-doped TiO_2. However, the EXAFS results unambiguously demonstrate that the second phase α-Fe_2O_3 appear in the Fe-doped TiO_2 with 5 wt% iron content. In fact, α-Fe_2O_3 species are probably much smaller clusters with high dispersion on the surface of TiO_2. With the XRD technique it is difficult to detect the diffraction signals when the sizes of crystalline grains are small enough. This is the possible reason for the absence of the α-Fe_2O_3 peaks. Kim *et al.* [9] have also reported that the secondary phase Fe_3O_4 exists in 7% Fe-doped TiO_2 prepared by OPA-MBE, by using XMCD and XANES techniques. This indicates that different secondary phases easily form in the highly doped Fe-TiO_2 prepared by different preparation methods. We consider that the existence of the secondary phase is the possible reason for explaining that the magnetic moment values per Fe atoms claimed in Refs [5] and [6] are different.

CONCLUSIONS

In summary, we have investigated the local structure around iron in anatase TiO_2 by using EXAFS technique. We find that for the sample with low iron content (1 and 2 wt%), the iron ions are incorporated into the lattice of anatase, and substitute the Ti ions. With the iron content increasing to 5 wt%, only part of iron ions enter the lattice of anatase, and the rest form α-Fe_2O_3 phase. As the iron content reaches 10 wt%, iron ions mainly exist in α-Fe_2O_3 phase. No oxygen vacancy is detected around iron ions substituting the Ti ions. Iron ions occupying the Ti sites greatly change the symmetry of the first Fe-O shell.

ACKNOWLEDGEMENTS

We thank the Beijing Synchrotron Radiation Facility for giving us the beam time for the XAFS measurement. This work is supported by National Science Foundation of China (Grant No.10275061).

REFERENCES

1. S. DasSarma, *Science* **289**, 516 (2001).
2 S. A. Wolf, D. D. Awschalom, R. A. Buhrman, J. M. Daughton, S. Von. Molnar, M. L. Roukes, A.Y. Chtchelkanova, and D. M. Treger, *Science* **294**, 1488 (2001).
3. Min Sin Park and B. I. Min, *Phys. Rev. B* **68**, 033202 (2003).
4. Z. J. Wang, W. D. Wang and J. Tang, *Appl. Phys. Lett.* **83**, 518 (2003).
5. R. Suryanarayanan, V. M. Naik, P. Kharel, P. Talagala and R. Naik, *J. Phy.: Condens. Matter*. **17**, 755 (2005).
6. N. Hong, W. Prellier, J. Sakai and A. Hassini, *Appl. Phys. Lett.* **84**, 2850 (2004).
7. X. H. Wang, J. G. Li, H. Kamiyama, M. Katada, N. Ohashi, Y. Moriyoshi and T. Ishigaki, *J. Am. Chem. Soc.* **127**, 10982 (2005).
8. A. B. Bally, E. N. Korobeinikova, P.E. Schmid, F. Levy and F. Bussy, *J. Phys. D: Appl. Phys.* **31**, 1149 (1998).
9. Y. J. Kim, S. Thevuthasan, T. Droubay, A. S. Lea, C. M. Wang, V. Shutthanandan, R. P. Sears, B. Talor and B. Sinkovic, *Appl. Phys. Lett.* **84**, 3531 (2004).
10. S. Y. Zhu, Y. Z. Li, C. Z. Fan, D. Y. Zhang, W. H. Liu, Z. H. Sun and S. Q. Wei, *Physica B* **364**, 199 (2005).
11. E. A. Stern, M. Newville, B. Ravel, D. Haskel and Y. Yacoby, *Physica B* **208**, 117 (1995).
12. S. I. Zabinsky, J. J. Rehr, A. Ankudinov, A. L. Albers and M. J. Eller, *Phys. Rev. B* **52**, 2995 (1995).